ARTICLE

Adsorption and Lubricating Properties of Poly(L-lysine)-*graft*-poly(ethylene glycol) on Human-Hair Surfaces

Seunghwan Lee,[†,‡] Stefan Zürcher,[†] Antoine Dorcier,[†] Gustavo S. Luengo,*[,§] and Nicholas D. Spencer*[,†]

Laboratory for Surface Science and Technology, Department of Materials, ETH Zurich, Wolfgang-Pauli-Strasse 10, CH 8093 Zurich, Switzerland, and L'Oréal Recherche, 1 Avenue Eugène Schueller, 93601 Aulnay-Sous-Bois, France

ABSTRACT We have characterized the adsorption and lubricating properties of the polycation−PEG graft copolymer poly(L-lysine)-*graft*-poly(ethylene glycol) (PLL-*g*-PEG) on human-hair surfaces by means of X-ray photoelectron spectroscopy (XPS), fluorescence microscopy, and atomic force microscopy (AFM). XPS measurements indicated that PLL-*g*-PEG copolymers spontaneously adsorbed onto the surface of bleached-hair samples (a good model of a weathered, damaged hair surface for cosmetic care applications) from an aqueous solution. Further treatment with cationic surfactants present in common shampoo formulations removed the adsorbed PLL-*g*-PEG from the hair samples. Fluorescence microscopy showed that the adsorption of PLL-*g*-PEG onto the hair samples from an aqueous polymer solution occurred inhomogeneously. Nanotribological studies with AFM (friction vs load plots) revealed that the relationship between load and friction was approximately linear for all hair samples, while the slopes of the plots varied considerably along the hair sample surface. Under ambient, "dry" conditions, the frictional properties of the bleached, bleached + PLL-*g*-PEG-treated, and bleached + PLL-*g*-PEG-treated and subsequently surfactant-treated hair samples did not reveal a clear difference. In distilled water, however, the bleached + PLL-*g*-PEG-treated hair samples showed statistically lower frictional properties than simply bleached or bleached + PLL-*g*-PEG-treated and subsequently surfactant-treated hair samples. Overall, the three instrumental techniques have consistently shown that the adsorption of PLL-*g*-PEG onto the hair sample surface occurs unevenly, which can be ascribed to the intrinsically heterogeneous properties of the human-hair surface. A control experiment, involving an injection of concentrated PLL-*g*-PEG solution into a liquid cell where an AFM tip was already scanning over a specific area (line scan mode), revealed an immediate and apparent reduction in the frictional force. Despite the inhomogeneity of the hair surface, the adsorption of the polymer seems to be extremely effective in promoting lubrication of the fiber. This suggests that the adsorbed graft copolymers act as a boundary lubricant on the hair surface. The presence of a more organized, brushlike layer of polymers contrasts with the usual random adsorption of chains that is believed to be present in the case of linear polyelectrolytes that are nowadays applied for shampoos and conditioners in the cosmetic or textile industries.

KEYWORDS: PLL-*g*-PEG • hair • lubrication • adsorption • water

1. INTRODUCTION

Poly(L-lysine)-*graft*-poly(ethylene glycol) (PLL-*g*-PEG) is a family of graft copolymers comprising a polycationic PLL backbone with PEG side chains, and it is known to provide an effective approach to end-grafting a dense, "brushlike" layer of PEG chains onto a variety of surfaces (1−14). This approach is particularly efficient for negatively charged surfaces, such as many metal−oxide surfaces in neutral aqueous solutions (1−4, 6−11) because the positively charged PLL backbones are attracted to the substrates by electrostatic interaction and thus act as anchoring groups, while grafted PEG side chains extend into the bulk aqueous solution to maximize their interaction with water. The molecular structure and conformation of PLL-*g*-PEG at the water/oxide interface are illustrated in Figure 1. As is well known, surface-grafted, "brushlike" PEG layers can impart unique resistance to nonspecific adsorption of proteins (1−4, 15−17) or bacteria (5, 18), stabilization of suspensions (19, 20), and lubricating properties (6−11, 21) to surfaces in an aqueous environment. The latter point is particularly important in tribological applications in which water-based lubrication is either unavoidable, such as in biomedical applications (13, 22), or desirable, such as in nonferrous bearing systems applied in the food or pharmaceutical industries (13, 14).

We have investigated the properties of PLL-*g*-PEG as an adsorbing layer to impart lubricity to the surface of keratin-based natural fibers, in particular human hair. Such surfaces (wool is another well-studied keratin fiber) are very complex and inhomogeneous, in both their morphological and chemical properties (24−30), because they are essentially composed of proteins and therefore include a variety of chemical

* To whom correspondence should be addressed. Tel: +41 44 632 68 50 (N.D.S.), +33 1 58317173 (G.S.L.). Fax: +41 44 633 10 27 (N.D.S.), +33 1 48689924 (G.S.L.). E-mail: spencer@mat.ethz.ch (N.D.S.), gluengo@rd.loreal.com (G.S.L.).

Received for review May 16, 2009 and accepted July 30, 2009

† ETH Zurich. E-mail: stefan.zuercher@mat.ethz.ch (S.Z.), antoine.dorcier@gmail.com (A.D.).

‡ Present address: Department of Mechanical Engineering, Technical University of Denmark, Kemitorvet, 2800 Kgs. Lyngby, Denmark. E-mail: seele@mek.dtu.dk.

§ L'Oréal Recherche.

DOI: 10.1021/am900337z

Published on Web 08/26/2009

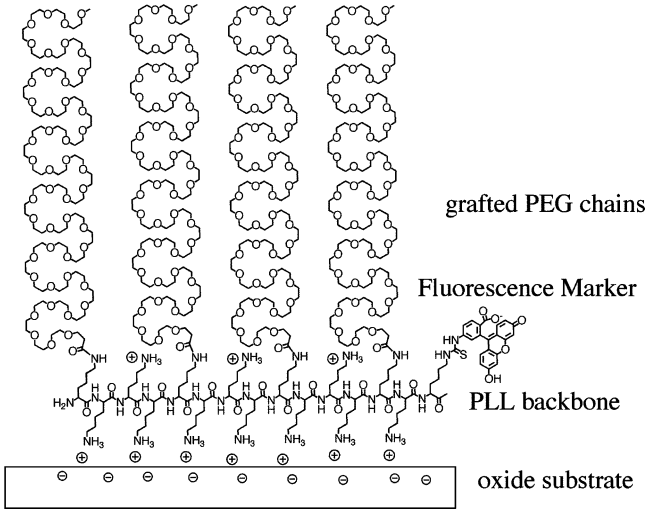

FIGURE 1. Sketch of the molecular structure of PLL-*g*-PEG and its conformation on a negatively charged surface in an aqueous environment. If present, fluorescence markers are covalently, but randomly linked with the PLL backbone at a ratio of roughly 1 chromophore per 25 lysine monomers (shown in the figure is the case for RBITC, but this is also applicable to 5-FITC). The PEG chains in reality will have a random-coil configuration and are not ordered as depicted in this sketch.

functional groups in their side chains (sulfonate, carboxylate, hydroxyl, amine, disulfide, thioether, aromatic, alkyl, etc.) (24−28). In addition, a number of fatty acids are known to be present on the outermost surface of human hair (28−30). Despite this complexity, the human-hair surface is known to display net negative charges in a neutral aqueous environment, with an isoelectric point of ca. 3.7 (24, 25) primarily because of the presence of strongly anionic sulfonate groups on the keratin surface, particularly in bleached or weathered hair. In addition, the surface of the cuticle scales has been proven to be rather smooth (roughness ∼10−30 nm) on a local scale (28, 29). Thus, as shown with many other cationic species in previous studies (24, 25), PLL-*g*-PEG is expected to readily adsorb onto the human-hair surface from an aqueous solution via electrostatic attraction.

Most of what is known about the conditioning technologies used in current shampoos and conditioners relies on the adsorption of polymers to the hair surface. Previous work on hair-lubricating agents has mainly involved highly charged species such as polyelectrolytes (i.e., quaternary ammonium derivatives of hydroxyethyl cellulose) (31), although silicones are also used (32). These conditioning agents are believed to adsorb in a random-coil conformation on the hair surface (33), providing good cosmetic performance, or good processing properties, in the case of wool. The specific brushlike structure exhibited by PLL-*g*-PEG when adsorbed onto model surfaces is the cause of its well-known lubricating properties, and its adsorption on hair allows one to study how this structure is preserved on a more complex, natural fiber. This is also a new technological approach to the lubrication and protection of keratin natural fibers on the nanostructural level.

To investigate the adsorption and lubricating properties of PLL-*g*-PEG, we have employed several surface-analytical approaches that are compatible with hair surfaces, namely, X-ray photoelectron spectroscopy (XPS), fluorescence microscopy, and atomic force microscopy (AFM). While the first two techniques served to characterize the adsorption behavior of PLL-*g*-PEG onto hair surfaces, AFM has been mainly employed to characterize the local lubricity provided to the hair surface by the copolymers, because of its intrinsic submicrometer-scale mechanical contact with the sample surface (27−29, 34−40).

2. MATERIALS AND METHODS

2.1. Hair Sample Preparation. Three types of hair samples have been prepared: (a) bleached hair, (b) poly(L-lysine)-*graft*-poly(ethylene glycol) (PLL-*g*-PEG)-treated hair, and (c) hair treated with surfactant following PLL-*g*-PEG treatment (denoted as "shampooed hair").

(a) Native whole tresses (25 cm in length and 250 mg in weight) were obtained from a female Caucasian, 90% blond, taken at 1−2 cm distance from the scalp. There followed an oxidative laboratory treatment with 110-volume hydrogen peroxide (H_2O_2) for ∼10 min without agitation. These are denoted as "bleached" hair samples or simply "hair" samples below and mimic weathered, damaged hair conditions close to normal natural aggressions.

(b) A tress of bleached hair was selected and washed with 50 cm^3 of 1% aqueous sodium dodecylsulfate (Aldrich, 2 wt % solution) for 2 min, followed by copious rinsing with double-distilled water and careful drying in a nitrogen stream. Treatment of these damaged hair samples with PLL-*g*-PEG was carried out by simply dipping the samples into 400 mg of an aqueous solution containing PLL-*g*-PEG (5 wt % in distilled water) for 30 min at 60 °C, followed by rinsing with distilled water and drying in ambient conditions.

(c) "Shampooed hair" samples were prepared by shampooing of the PLL-*g*-PEG-treated hair samples for approximately 2 min with a commercial shampoo (containing foaming anionic, amphoteric, and nonionic surfactants and various oils, cationic polymers, silicones, etc., for cosmetic effects) and subsequent rinsing with distilled water and drying in ambient conditions.

All of the following experiments were carried out at ambient temperature (ca. 20 °C). However, before use, all of the hair samples were stored in a refrigerator (2−8 °C).

2.2. PLL-*g*-PEG and Fluorescence-Labeled PLL-*g*-PEG. PLL-*g*-PEG was synthesized by reaction of the *N*-hydroxysuccinimidyl ester of methoxy(ethylene glycol) propionic acid (mPEG-SPA, Nektar, Huntsville, AL) with the amino groups of poly(L-lysine) hydrobromide (Sigma, St. Louis, MO) at a controlled stoichiometric ratio. Details on the synthesis and analytical information are available in previous publications. (1−3) The PLL-*g*-PEG used in this work, denoted as "PLL(20)-*g*[3.4]-PEG(5)" (3, 9−11), has a molecular weight of 20 000 g/mol for the PLL backbone (including HBr as a precursor), 5000 g/mol for PEG side chains, and a grafting ratio of 3.4 (lysine-mer/PEG side chains). Thus, on average, every 3.4 lysine units carry a PEG side chain with 113 EG units. The nonfunctionalized lysine units are protonated at pH 7 and therefore are responsible for binding to negatively charged surfaces. The polydispersities of the reagents, M_w/M_n, are 1.2 and 1.1 for the PLL backbone and PEG side chains, respectively.

For fluorescence microscopy experiments, PLL-*g*-PEG was labeled by one of the two fluorescence markers: rhodamine B isothiocyanate (RBITC, red) or fluorescein 5-isothiocyanate (5-FITC, green) (Fluka, Switzerland). The PLL-*g*-PEG copolymers labeled with the fluorescence markers are denoted as PLL-*g*-PEG* (RBITC) and PLL-*g*-PEG† (5-FITC). Both fluorescence markers are isothiocyanate-activated chromophores that react covalently with the PLL backbone through a thiourea linkage. The fluorescence markers were added in a ratio of roughly 1 chromophore per 25 lysine monomers, i.e., 3.7 per PLL-*g*-PEG

molecule, on average. In brief, the polymer (0.37 mmol of total lysine concentration) was dissolved in a borate buffer (3.5 mL), and either RBITC (6 mg, 0.011 mmol) or 5-FITC (4.2 mg, 0.011 mmol) dissolved in *N*,*N*-dimethylformamide (0.3 mL) was added with vigorous stirring. After reacting for 16 h at room temperature, the reaction solution was dialyzed (Spectrapore dialysis membrane MWCO 12000−14000) against pure water to remove unreacted fluorescence markers and reaction side products. The dialysis water was exchanged until colorless (a total of three times over a period of 3 days) (11). A schematic illustration of PLL-*g*-PEG with the RBITC fluorescence marker is shown in Figure 1.

2.3. XPS. XPS analyses were performed using a PHI 5700 spectrophotometer equipped with a concentric hemispherical analyzer (CHA; Physical Electronics, Eden Prairie, MN). Spectra were acquired at a base pressure of 10^{-8} mbar or below using a nonmonochromatic Al Kα source operating at 350 W and positioned 10 mm away from the sample. The instrument was run in the minimum-area mode using an aperture of 0.4 mm diameter. The CHA was used in the fixed-analyzer-transmission mode. Pass energies used for survey scans and detailed scans were 187.85 and 23.5 eV, respectively, for carbon C 1s, oxygen O 1s, nitrogen N 1s, calcium Ca 2p, and sulfur S 2p. Under these conditions, the energy resolutions (full width at half-maximum height, fwhm) measured on silver Ag $3d_{5/2}$ are 2.7 and 1.1 eV, respectively. Acquisition times were approximately 5 min for survey scans and 15 min (total) for high-energy-resolution elemental scans. These experimental conditions were chosen in order to have an adequate signal-to-noise ratio in a minimum time and to limit beam-induced damage. In addition, the sample holder was cooled with liquid nitrogen to reduce outgassing of the highly hydrated samples. The measurements were performed with a takeoff angle (detection angle to the surface) of 45° with respect to the sample-holder plane. All recorded spectra were referenced to the aliphatic hydrocarbon C 1s signal at 285.0 eV. Data were analyzed with the program *CasaXPS* [version 2.3.5, www.casaxps.com]. The signals were fitted using Gaussian−Lorentzian functions and least-squares-fit routines following Shirley iterative background subtraction. Sensitivity factors were calculated using published ionization cross sections (41) corrected for the energy dependence of the transmission function of the instrument and the attenuation-length dependence on kinetic energy.

A bundle of hairs was stretched over a 2.5-cm-diameter recessed sample holder to avoid signals arising from any underlying material. Up to three different measurements were performed on each bundle of hairs. Only one type of hair was introduced per analytical run to avoid X-ray degradation of waiting samples.

2.4. Fluorescence Microscopy. A fluorescence microscope (Zeiss Axiovert 135 TV, Carl Zeiss, Berlin, Germany) equipped with a CCD camera (ORCA-ER, Hamamatsu, Japan) was employed to visualize the adsorption of PLL-*g*-PEG on the surface of the hair samples. As described above, PLL-*g*-PEG copolymers from the same batch were marked by rhodamine B isothiocyanate (RBITC) or fluorescein 5-isothyocyanate (5-FITC). RBITC absorbs light at 555 nm and emits at 576 nm (red). These wavelengths were filtered out with a Zeiss Filter-set No. 15. 5-FITC absorbs light at 490 and 494 nm and re-emits light at 520 and 525 nm (green). These wavelengths were filtered out with a Zeiss Filter-set No. 10. Similar to the treatment with unlabeled PLL-*g*-PEG, the hair samples were immersed in an aqueous solution containing fluorescently labeled PLL-*g*-PEG, 5 wt % in pure water for 30 min, and subsequently rinsed with pure water and dried under a stream of nitrogen.

2.5. AFM. A commercial atomic force microscope (Dimension 3000, Digital Instruments, Santa Barbara, CA) was employed to characterize the surface-morphological and frictional properties of the hair samples. Commercial V-shaped, silicon nitride tip/cantilever assemblies (model NP-S, Veeco Instruments, Santa Barbara, CA) were employed (average length = 196 μm, width = 41 μm, thickness = 0.6 μm, as provided by the manufacturer). The spring constant provided by the manufacturer, 0.12 N/m, was employed to estimate the applied load. The raw voltage signal (mV) was used to compare friction forces. The AFM tip/cantilever assembly was cleaned by immersion in a commercial cleaner (Roche "Cleaner", 300 mmol/L hydrochloric acid and 1% detergent) and in distilled water, in sequence (10 min each). To avoid any contamination during the sample preparation, hair samples were handled with latex-gloved hands and tweezers (stainless steel) only.

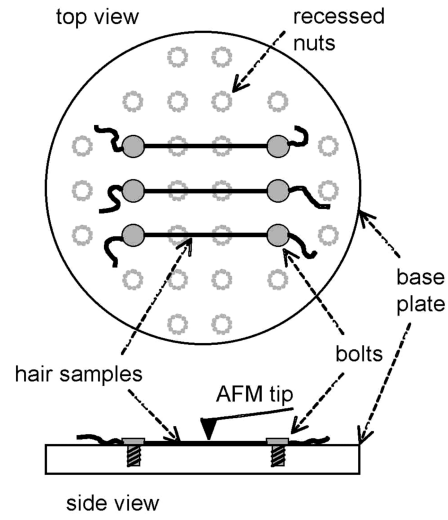

FIGURE 2. Sketch of the hair sample holder used in liquid-mode AFM experiments. Base plates and bolts are made of stainless steel.

Fixing hair fibers onto a sample holder to provide mechanical stability is of critical importance for meaningful AFM measurements. To this end, individual hair fibers were stretched on a silicon wafer, with both ends being glued down using nail polish, which has an advantage over epoxy in that it does not spread during hardening (38). The length of the fixed hair fiber was about 3 cm. This approach provided sufficient mechanical stability for measurements to be carried out under ambient air conditions. In water, however, hair samples fixed onto a sample holder in this way were much more mobile. Thus, a special, yet simple, hair sample holder, constructed of a stainless steel plate, screws, and nuts, was designed to improve mechanical stability (Figure 2). Distilled water was used to provide the aqueous environment during measurements. For all AFM experiments, the placement of the cantilever/tip assembly onto hair surfaces was aided by an optical microscope, which is integrated with the AFM.

3. RESULTS AND DISCUSSION

3.1. XPS. On each hair sample, a survey spectrum was measured with low resolution, in order to detect all elements present. As expected, the main elements were oxygen, nitrogen, carbon, and sulfur. In addition, trace amounts of calcium and silicon, which are commonly present in hair, according to the literature (24, 25), were also detected. Following the survey spectrum, high-resolution spectra of the detected elements were measured and analyzed. Among the three hair samples (bleached, shampooed, and PLL-*g*-PEG-treated), no significant differences were observed in the oxygen, nitrogen, and sulfur signals. However, a significant difference was observed in the C 1s signal. Multiple measurements (at least three) carried out for each type of hair

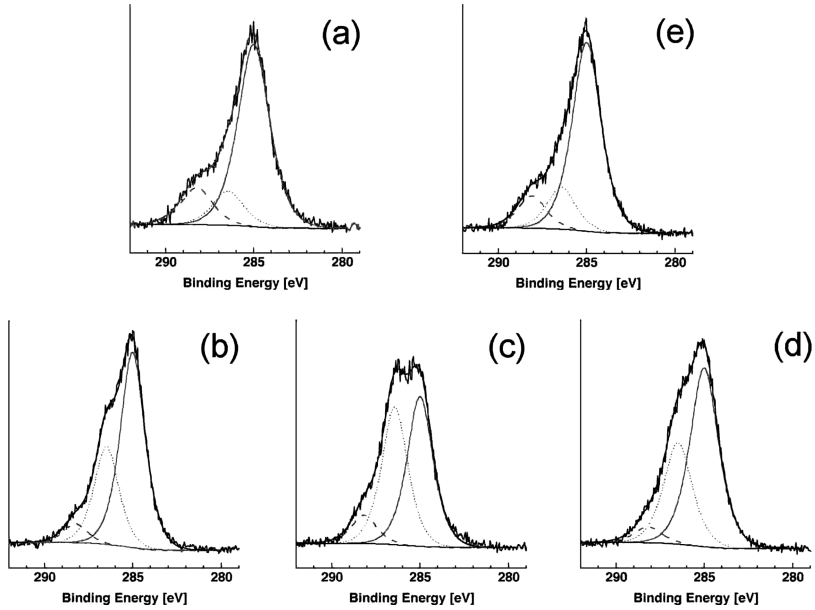

FIGURE 3. C 1s peak of the three types of hair samples: (a) bleached hair; (b−d) PLL-*g*-PEG-treated hair; (e) shampooed hair following PLL-*g*-PEG treatment. The gray dashed lines (288.2 ± 0.1 eV) represent the carbon signal from N−C═O, the gray dotted lines (286.5 ± 0.1 eV) that from C−O and C−N, and the gray solid lines (285 eV) that from aliphatic carbons.

sample showed that the acquired spectra for the bleached and shampooed hair sample are quite reproducible, whereas those for the PLL-*g*-PEG-treated samples are noticeably different for each run. For this reason, we present single, representative data for the bleached (Figure 3a) and shampooed (Figure 3e) hair samples and all three spectra for the PLL-*g*-PEG hair samples (Figure 3b−d).

The C 1s spectrum can be deconvoluted into three major components: (i) N−C═O with a binding energy of 288.2 ± 0.1 eV (gray dashed lines), (ii) C−O and C−N with a binding energy of 286.5 ± 0.1 eV (gray dotted lines), and (iii) aliphatic carbon with a binding energy of 285 eV (gray solid lines, internal reference). On the PLL-*g*-PEG-treated hair samples (Figure 3b−d), the contribution from C−O/C−N (gray dotted lines) was higher than that of the bleached hair samples (Figure 3a) for all three cases. Among three different spots of PLL-*g*-PEG-coated hairs, different amounts of C−O and C−N peaks were detected, which is probably associated with the inhomogeneous coating of the copolymer on the hair sample surface. The higher signals of the C−O and C−N peaks for the PLL-*g*-PEG-treated hair samples, compared to the bleached hair samples (Figure 3a) are most probably due to the PEG chains (C−O) in PLL-*g*-PEG. The spectra obtained from the shampooed hair (Figure 3e) after PLL-*g*-PEG treatment appeared almost identical with those of bleached hair samples (Figure 3a).

The XPS observations suggest that PLL-*g*-PEG copolymers spontaneously adsorb from an aqueous solution onto the bleached hair samples, and yet virtually all of the adsorbed polymers are removed by shampooing.

3.2. Fluorescence Microscopy. The hair samples treated with fluorescently labeled PLL-*g*-PEG were characterized by fluorescence microscopy. In parallel, untreated hair samples were examined as a reference. Excitation by 490 and 494 nm light led to the emission of green light from both

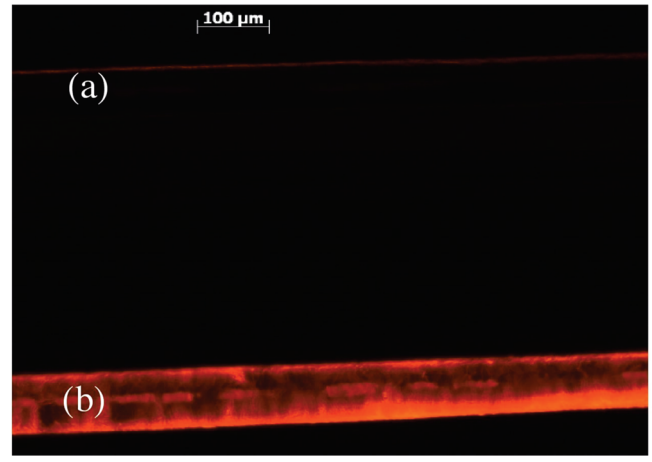

FIGURE 4. Fluorescence microscopic images of (a) a bleached hair sample and (b) a bleached hair sample treated with RBITC-labeled PLL-*g*-PEG.

bleached and PLL-*g*-PEG†-treated hair samples, and thus it did not allow the determination of PLL-*g*-PEG adsorption onto the hair samples. On the other hand, as shown in Figure 4, a bleached hair sample and a hair sample treated with PLL-*g*-PEG* showed a clear difference in fluorescence microscopic images; (a) a bleached hair sample (upper) showed nearly no emission and (b) a PLL-*g*-PEG*-treated hair sample (lower) showed strong emission of red fluorescence. This observation implies that PLL-*g*-PEG spontaneously adsorbs from an aqueous solution onto hair surfaces. A close examination of the PLL-*g*-PEG*-treated hair sample reveals that the fluorescence intensity is inhomogeneously distributed along the hair; this observation is consistent with the XPS results, suggesting that adsorption of PLL-*g*-PEG occurs in an inhomogeneous manner.

3.3. AFM. ***3.3.1. Characterization of Frictional Properties of Hair Surfaces by Means of AFM.*** Human-hair fiber is covered with partially overlapping cuticle

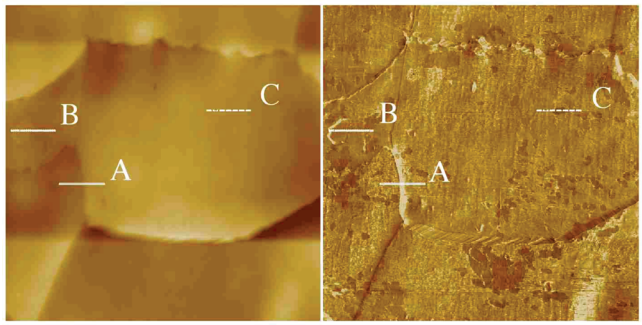

FIGURE 5. Representative AFM topographic (left) and lateral-force (right) images (10 μm × 10 μm), revealing the inhomogeniety of the surface properties. The cursor lines, A−C, are shown to explain the procedure of acquiring "valid" friction data (line-scan mode); briefly, the regions excluding the topographic contribution to frictional properties only, such as C, are considered for the evaluation of the intrinsic frictional properties of the hair samples, whereas the regions revealing severe convolution of the topography with frictional properties, such as A and B, are discarded.

layers. This feature was readily verified by obtaining the topographic images of the hair sample surfaces with AFM on a scale larger than ca. 10 μm × 10 μm. A representative example is shown in Figure 5a. In Figure 5b, a simultaneously obtained lateral-force image, which represents the distribution of frictional properties over the selected area, is also presented. For the morphology and lateral-force images, the level of brightness scales with the magnitude of the height or the friction force, respectively.

A comparison of the morphology (Figure 5a) and lateral-force images (Figure 5b) reveals several points that need to be carefully considered for friction studies on hair samples in this work. First, the boundaries between cuticle layers often show distinctively different frictional properties compared with their surroundings, for instance, as shown in line A in Figure 5. Because the friction signals are obtained by monitoring the lateral twisting of the tip/cantilever assembly in AFM, this feature is strongly associated with abrupt changes in the topography at steps or valleys at domain boundaries. For this reason, we consider that this feature does not represent the intrinsic frictional properties of human-hair surfaces and the boundaries between cuticle layers were excluded from friction measurements. Second, even in the region away from the boundaries between cuticles, i.e., within a single cuticle layer, significant frictional inhomogeneity is often observed; in some cases, such features apparently result from nanoscale local asperities, as exemplified by line B in Figure 5. However, in some other cases, such features arise for reasons other than local asperities, such as chemical inhomogeneity of the sample surface, as seen for line C in Figure 5. In this work, if the topographic corrugation of a selected line scan was within ca. ±5 nm, the observed friction data were considered valid, representing the intrinsic frictional properties of the hair samples, excluding the influence of topographic features. However, if a selected line scan includes random local asperities higher than ±5 nm, the corresponding friction data were discarded.

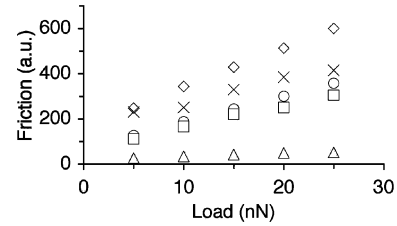

FIGURE 6. "Friction vs load" plots obtained from a bleached hair sample under ambient air conditions [the five symbols represent the average friction forces (out of 10 measurements for a fixed position and under a fixed load) obtained from five different positions along the hair sample].

Having excluded excessive topographic corrugations, frictional forces along the selected line were measured by taking the difference in the friction signals between scanning in opposite directions, i.e., "line-scan mode" (Veeco Instruments, Santa Barbara, CA), under fixed load and speed. Adhesive forces were not included in the definition of the load. The scan length was 500 nm, and the scan rate was 1 Hz. The same procedure can be repeated by varying the load [from low (5 nN) to high (25 nN)] by means of setting varying set points, yielding "friction vs load" plots.

3.3.2. Lubrication Properties under Ambient Conditions. The frictional properties of the hair samples were initially characterized under ambient conditions. The sequence of data acquisition was as follows; first, one specific location (line) was selected from one hair sample, and if the morphology was sufficiently smooth (the height corrugation less than 5 nm) as described in section 3.3.1, then the friction data were acquired under varying loads during line scans. The scan direction was always along the hair sample. At each load, friction forces were measured 10 times, and average values were obtained. This procedure was repeated for different locations (lines) along the hair sample. A representative friction vs load plot for the bleached hair sample is shown in Figure 6. In this plot, five different symbols (circle, square, triangle, diamond, and cross) represent the average friction forces obtained from five different locations from a single hair sample. While the relationship between friction and load was observed to be fairly linear for all cases, the magnitude of frictional forces varied very significantly from one position to another.

Because topographical contributions to friction forces were excluded in the friction measurements, the highly scattered frictional properties observed from the bleached hair sample surfaces, reflected from both the lateral force images (e.g., Figure 5b) and the "friction vs load" plots (e.g., Figure 6), are believed to reflect the inhomogeneous chemical nature of the hair sample surface. There was no particular correlation between the observed frictional properties and the location along the hair sample surface (e.g., near the root, middle, or near the end) or the sequence of measurements.

In order to obtain more statistical information, the same measurements were repeated for four different bleached hair samples. Then, the entire procedure was repeated on PLL-*g*-PEG-treated hair samples, followed by shampooed hair samples. Prior to the start of measurements and between the measurements of the different types of hair samples, the

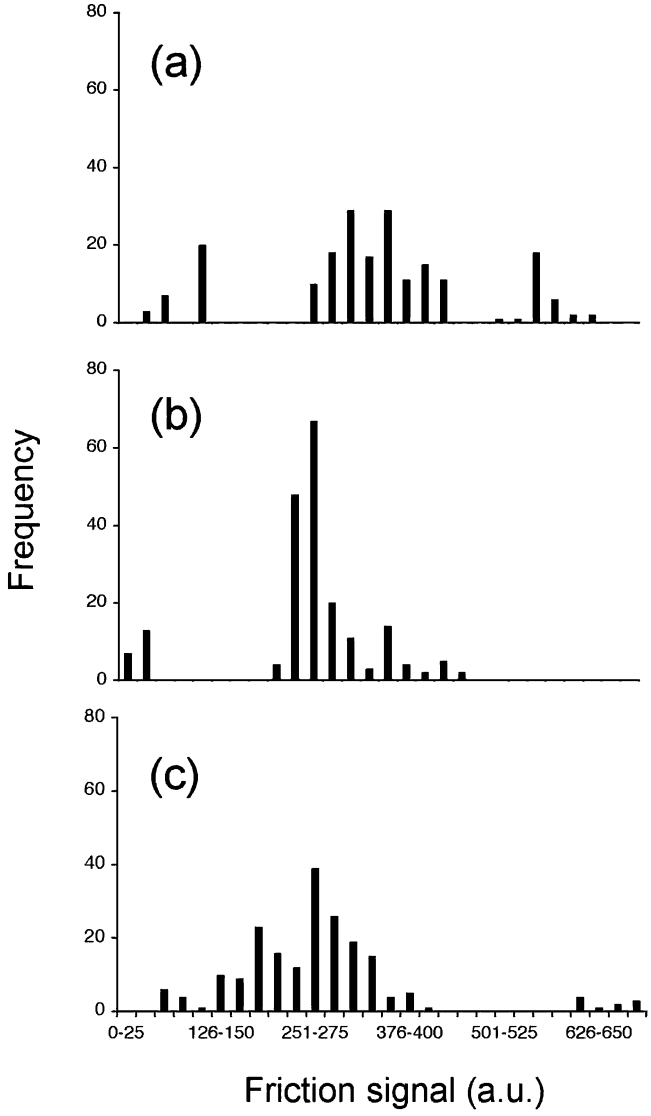

FIGURE 7. Statistical distribution of friction signals obtained under 25 nN in ambient air conditions for three different types of hair samples: (a) bleached; (b) PLL-*g*-PEG-treated; (c) shampooed.

AFM tip was cleaned as described in section 2.4. The distribution of frictional forces obtained under 25 nN, which showed the highest contrast, is shown in Figure 7 (4 hairs × 5 spots × 10 measurements = 200 total data points for each type of hair sample). Average frictional forces and standard deviations (from Figure 7) are presented in Figure 8. A few characteristics are immediately apparent: First, regarding the frequency, very high friction forces (>500) are observed only in the bleached and shampooed hair samples. Second, the peak for the most probable friction is very similar for the PLL-*g*-PEG-treated and shampooed hair samples, and that for bleached hair is only slightly higher than the others. Third, there is a tendency for the average friction forces (Figure 8) to shift to lower values in the order of bleached (342.5 ± 142.5), shampooed (268.9 ± 118.2), and PLL-*g*-PEG-treated hair samples (255.7 ± 94.4), yet standard deviations are too high for any significance to be drawn.

Overall, on the basis of the data obtained under ambient conditions, it is difficult to assert that the PLL-*g*-PEG coating

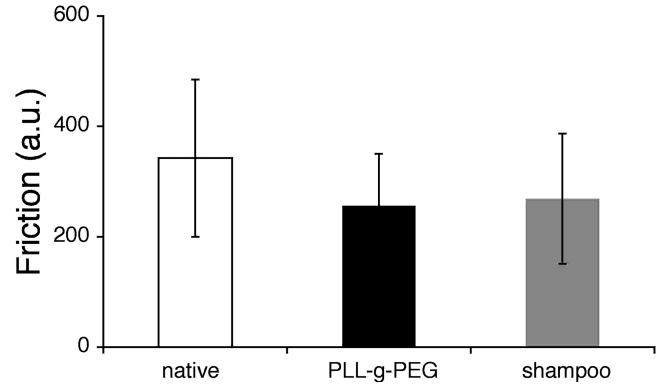

FIGURE 8. Average friction signals (from Figure 7) obtained under 25 nN in ambient air for three different types of hair samples (bleached, PLL-*g*-PEG-treated, and shampooed). Error bars represent the standard deviations over 200 measurements (4 hair fibers × 5 positions × 10 measurements per each type of hair sample).

of the hair sample surface modifies the lubrication of hair sliding against a nanoscopic silicon nitride AFM tip.

3.3.3. Lubrication Properties in Water. Friction measurements in water were carried out in the same manner as for the ambient measurements. An AFM tip/cantilever assembly, which was different in force sensitivity from that used for the measurements in ambient conditions (despite the fact that the spring constants are identical, 0.12 N/m, as provided by the manufacturer), was used for all of the friction measurements of the hair samples in water. Thus, it should be noted that, although the data obtained in water showed generally smaller numerical values than those in ambient conditions (see below), no direct comparison should be made between two groups of the data. In these measurements, three hair fibers were selected for each hair sample. Thus, the total number of data points for each load for one type of sample was 150 (3 fibers × 5 spots × 10 measurements). The statistical distributions of the friction forces for the bleached, PLL-*g*-PEG-treated, and shampooed hair samples are shown in Figure 9. Average friction forces and standard deviations are presented in Figure 10.

As with the results obtained from measurements in ambient conditions, the "friction vs load" plots obtained in water also showed a fairly linear relationship for all types of hair samples (data not shown). In addition, highly variable frictional properties along the hair sample surface were observed during measurements in water. However, these measurements revealed that in water PLL-*g*-PEG-treated hair samples exhibit statistically lower frictional properties than either bleached or shampooed hair samples.

Compared with the distribution of frictional forces under ambient conditions (Figure 7), there are some noticeable differences. First, there is a clear distinction between the most probable peaks in the friction signals for each hair sample; those from shampooed and bleached hair samples are roughly 2 or 3 times as large as those from PLL-*g*-PEG-treated hair samples, respectively. The order of the average friction force is also decreasing in the order bleached (225.7 ± 154.2), shampooed (215.3 ± 54.9), and PLL-*g*-PEG-treated (78.3 ± 45.5) hair. While there is some overlap between the standard deviations of bleached and PLL-*g*-PEG-treated hair

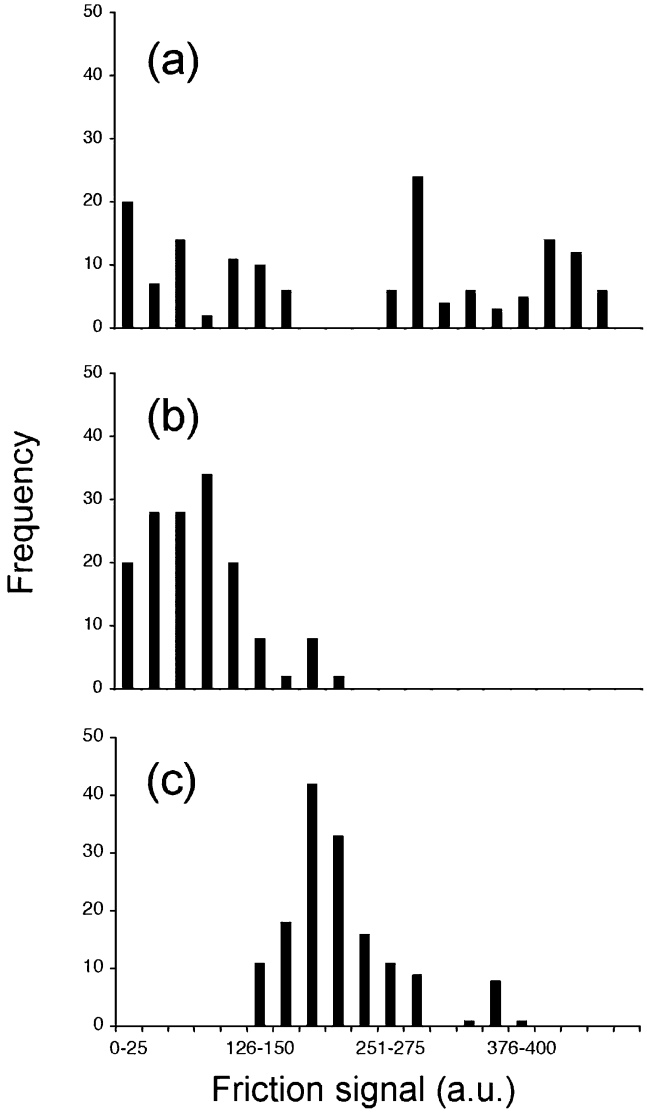

FIGURE 9. Statistical distribution of friction signals obtained under 25 nN in water for three different types of hair samples: (a) bleached; (b) PLL-*g*-PEG-treated; (c) shampooed.

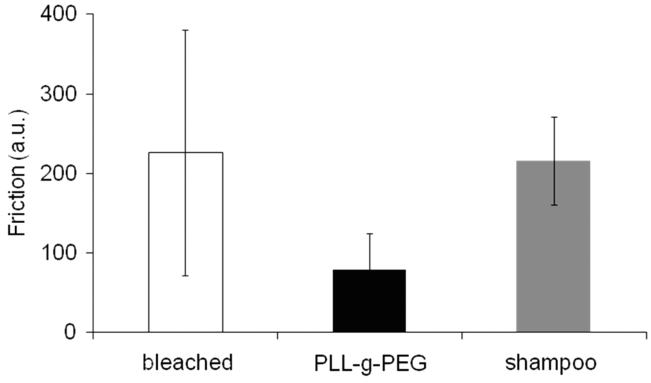

FIGURE 10. Average friction signals (from Figure 9) obtained under 25 nN in water for three different types of hair samples (bleached, PLL-*g*-PEG-treated, and shampooed). Error bars represent the standard deviations over 150 measurements (3 hair fibers × 5 positions × 10 measurements per each type of hair sample).

samples, frictional properties of PLL-*g*-PEG-treated hair samples are statistically much lower than the others, in contrast to the results in ambient conditions. This observation suggests that, in an aqueous environment, treatment with PLL-*g*-PEG renders the hair samples more lubricious.

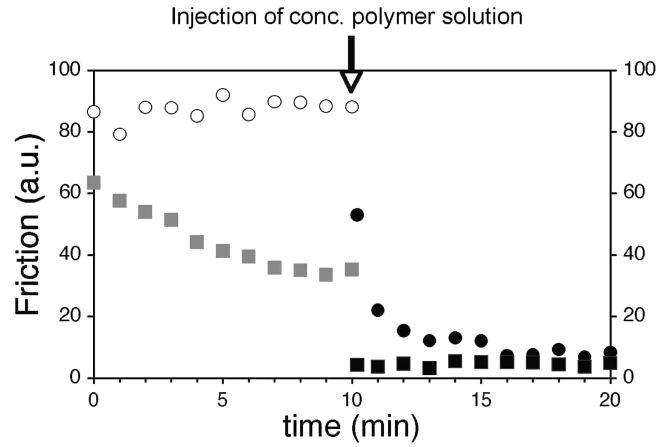

FIGURE 11. In situ friction measurements before (empty circles for the bare AFM tip and gray squares for the precoated AFM tip with PLL-*g*-PEG) and after (black circles for the bare AFM tip and black squares for the precoated AFM tip with PLL-*g*-PEG) injection of a concentrated PLL-*g*-PEG solution into the liquid cell in which the contact between the AFM tip and the hair sample occurs. The *x* axis represents the time and the *y* axis the friction signals, and as indicated by the arrow, injection occurred at ca. 10 min.

Frictional properties of PLL-*g*-PEG-treated, bleached, and shampooed samples in water are also highly scattered. This can be primarily ascribed to the inhomogeneous adsorption of PLL-*g*-PEG onto bleached hair samples, as suggested by data from XPS and fluorescence microscopy, and, in turn, to the inhomogeneous chemical nature, i.e., inhomogeneous distribution of negative charges, of bleached hair samples. To confirm the adsorption and lubricating properties of PLL-*g*-PEG on a hair sample surface in water, a control experiment was conducted as follows: while a new AFM tip was continuously scanning over a new bleached hair sample under a fixed load in a liquid cell (liquid volume ca. 50 mL), 1 mL of a concentrated PLL-*g*-PEG solution was injected into the cell. The final polymer concentration was ca. 0.25 mg/mL. As shown in Figure 11, where friction forces are plotted as a function of time, the friction signal was confirmed to be stable for ca. 10 min before injection of the concentrated polymer solution (friction signal was probed 10 times/min in the line-scan mode, and the average friction forces are presented in Figure 11). Thus, any change in the friction forces following injection of the polymer solution can be ascribed to the lubricating effect of PLL-*g*-PEG.

As shown by the circle symbols in Figure 11, injection of the PLL-*g*-PEG solution (at ca. 10 min along the *x* axis) induced a drastic and immediate reduction of the friction force. This behavior suggests that the adsorption and subsequent lubricating effect of PLL-*g*-PEG on a bleached hair sample surface is extremely rapid, as has been previously reported with other negatively charged surfaces (1−4, 6−11), as long as the adsorption occurs at all, as exemplified in this specific site on the bleached hair sample surface. However, because a bare AFM tip was employed in this measurement and because PLL-*g*-PEG is expected to adsorb onto silicon oxynitride as well, one can argue that the lubricating effect shown in Figure 11 (circle symbols) results from the PLL-*g*-PEG coating on the AFM tip side, not on the hair sample surface.

To exclude such a possibility, another control experiment was carried out using an AFM tip that was precoated with PLL-*g*-PEG and a bleached hair sample. Precoating of the AFM tip was carried out by immersing an AFM tip in a concentrated polymer solution for 15 min. As shown by the square symbols in Figure 11, an apparent improvement in the lubricating effect by injection of the PLL-*g*-PEG solution (at ca. 10 min along the *x* axis) was again observed.

4. CONCLUSIONS

We have characterized the adsorption and lubricating properties of a polycation−PEG graft copolymer, PLL-*g*-PEG, on human-hair surfaces by means of XPS, fluorescence microscopy, and AFM. Bleached hair samples, PLL-*g*-PEG-treated hair samples, and subsequently shampooed hair samples were studied. According to the XPS measurements, exposure of the bleached hair samples to an aqueous solution containing PLL-*g*-PEG appears to leave PLL-*g*-PEG on the surface of hair samples. Further treatment with shampoo, however, seems to remove the adsorbed PLL-*g*-PEG from the hair samples. Fluorescence microscopy clearly showed the spontaneous adsorption of PLL-*g*-PEG onto the bleached hair samples from an aqueous polymer solution. The load dependence of the frictional properties of the hair sample surfaces ("friction vs load" plots) has been characterized by lateral-force microscopy during sliding contact with the hair surfaces under controlled load (line-scan mode), both in ambient conditions and in a water environment. For all hair samples, the relationship between load and friction was approximately linear, yet the friction forces showed a highly scattered distribution along the hair sample surfaces. In ambient air conditions, the frictional properties of bleached, PLL-*g*-PEG-treated, and shampooed hair samples did not reveal a clear difference. In distilled water, however, PLL-*g*-PEG-treated hair samples showed statistically lower frictional properties than bleached or shampooed hair samples.

Most importantly, all three instrumental techniques have consistently shown that the adsorption of PLL-*g*-PEG onto hair sample surfaces takes place in an inhomogeneous manner, and this is ascribed to the intrinsically inhomogeneous surface properties, in particular the inhomogeneous distribution of negative charges, of human-hair surfaces. A control experiment revealed that injection of a concentrated PLL-*g*-PEG solution into the liquid cell, where a scanning AFM tip (line-scan mode) is confined to a local, specific area (line), led to an immediate and significant reduction in friction forces. Thus, it can be asserted that PLL-*g*-PEG does reduce the friction forces between the hair sample surfaces and the AFM tip in water within a local area where PLL-*g*-PEG can be readily adsorbed.

Acknowledgment. The authors thank their colleagues S. Vicic, P. Barbarat, and C. Cazeneuve at L'Oréal Recherche for kindly providing some of the samples and for fruitful discussions. We finally thank F. Leroy for his continuous support.

REFERENCES AND NOTES

(1) Kenausis, G. L.; Vörös, J.; Elbert, D. L.; Huang, N. P.; Hofer, R.; Ruiz, L.; Textor, M.; Hubbell, J. A.; Spencer, N. D. *J. Phys. Chem. B* **2000**, *104*, 3298–3309.
(2) Huang, N. P.; Michel, R.; Vörös, J.; Textor, M.; Hofer, R.; Rossi, A.; Elbert, D. L.; Hubbell, D. L.; Spencer, N. D. *Langmuir* **2001**, *17*, 489–498.
(3) Pasche, S.; De Paul, S. M.; Vörös, J.; Spencer, N. D.; Textor, M. *Langmuir* **2003**, *19*, 9216–9225.
(4) Morgenthaler, S.; Zink, C.; Städler, B.; Vörös, J.; Lee, S.; Spencer, N. D.; Tosatti, S. *Biointerphases* **2006**, *1*, 156–165.
(5) Maddikeri, R. R.; Tosatti, S.; Schuler, M.; Chessari, S.; Textor, M.; Richards, R. G.; Harris, L. G. *J. Biomed. Mater. Res. A* **2008**, *84*, 425–435.
(6) Lee, S.; Müller, M.; Ratoi-Salagean, M.; Vörös, J.; Pasche, S.; De Paul, S. M.; Spikes, H. A.; Textor, T.; Spencer, N. D. *Tribol. Lett.* **2003**, *15*, 231–239.
(7) Müller, M.; Lee, S.; Spikes, H. A.; Spencer, N. D. *Tribol. Lett.* **2003**, *15*, 395–405.
(8) Yan, X.; Perry, S. S.; Spencer, N. D.; Pasche, S.; De Paul, S. M.; Textor, M.; Lim, M. S. *Langmuir* **2004**, *20*, 423–428.
(9) Müller, M.; Yang, X.; Lee, S.; Perry, S. S.; Spencer, N. D. *Macromolecules* **2005**, *38*, 3861–3866.
(10) Müller, M.; Yang, X.; Lee, S.; Perry, S. S.; Spencer, N. D. *Macromolecules* **2005**, *38*, 5706–5713.
(11) Lee, S.; Müller, M.; Heeb, R.; Zürcher, S.; Tosatti, S.; Heinrich, M.; Amstad, F.; Pechmann, S.; Spencer, N. D. *Tribol. Lett.* **2006**, *24*, 217–223.
(12) Lee, S.; Spencer, N. D. *Science* **2008**, *319*, 575–576.
(13) Lee, S.; Spencer, N. D. In *Superlubricity*; Erdemir, A., Martin, J.-M., Eds.; Elsevier: Amsterdam, The Netherlands, 2007; Chapter 21, pp 365−396.
(14) Lee, S.; Spencer, N. D. *Tribol. Lett.* **2008**, *24*, 217–223.
(15) Harris, M. J. *Poly(ethylene glycol) chemistry biotechnical and biomedical applications*; Plenum Press: New York, 1992.
(16) Kingshott, P.; Thissen, H.; Griesser, H. J. *Biomaterials* **2002**, *23*, 2043–2056.
(17) Halperin, A. *Langmuir* **1999**, *15*, 2525–2533.
(18) Kingshott, P.; Wei, J.; Bagge-Ravn, D.; Gadegaard, N.; Gram, L. *Langmuir* **2003**, *19*, 6912–6921.
(19) Klein, J.; Luckham, P. F. *Macromolecules* **1984**, *17*, 1041–1048.
(20) Braithewaite, G. J. C.; Howe, A.; Luckham, P. F. *Langmuir* **1996**, *12*, 4224–4237.
(21) Raviv, U.; Frey, J.; Sak, R.; Laurat, P.; Tadmor, R.; Klein, J. *Langmuir* **2002**, *18*, 7482–7495.
(22) Kanika, C.; Lee, S.; Lee, B. P.; Dalsin, J. L.; Messersmith, P. B.; Spencer, N. D. *J. Biomed. Mater. Res. A* **2009**, *90*, 742−749.
(23) Bhushan, B. *Prog. Mater. Sci.* **2008**, *53*, 585–710.
(24) Stranick, M. A. *Surf. Interface Anal.* **1996**, *24*, 522–528.
(25) Beard, B. C.; Hare, J. *J. Surfact. Deterg.* **2002**, *5*, 145–150.
(26) Molina, R.; Jovancic, P.; Jocic, D.; Bertran, E.; Erra, P. *Surf. Interface Anal.* **2003**, *35*, 128–135.
(27) Baghdal, N.; Luengo, G. S. *J. Phys.: Conf. Ser.* **2008**, *100*, 052034, 1−4.
(28) Dupres, V.; Lagevin, D.; Guenoun, P.; Checco, A.; Luengo, G.; Leroy, F. *J. Colloid Interface Sci.* **2007**, *306*, 34–40.
(29) Breakspear, S.; Smith, J. R.; Luengo, G. *J. Struct. Biol.* **2005**, *149*, 235–242.
(30) Jones, L. N.; Rivett, D. E. *Micron* **1997**, *28*, 469–485.
(31) Qian, L.; Chariot, M.; Perez, E.; Luengo, G.; Potter, A.; Cazeneuve, C. *J. Phys. Chem. B* **2004**, *108*, 18608–18614.
(32) Hössel, P.; Dieing, R.; Nörenberg, R.; Pfau, A.; Sander, R. *Int. J. Cosmet. Sci.* **2000**, *22*, 1–10.
(33) Gruber, J. V.; Lamoureux, B. R.; Joshi, N.; Moral, L. *J. Cosmet. Sci.* **2001**, *52*, 131–136.
(34) Maxwell, J. M.; Huson, M. G. *Micron* **2005**, *36*, 127–136.
(35) Smith, J. R. *J. Microsc.* **1998**, *191*, 223–228.
(36) Breakspear, S.; Smith, J. R. *J. Microsc.* **2004**, *215*, 34–39.
(37) Sadaie, M.; Nishikawa, N.; Ohnishi, S.; Tamada, K.; Yase, K.; Hara, M. *Colloids Surf. B* **2006**, *51*, 120–129.
(38) McMullen, R. L.; Kelty, S. P. *Scanning* **2000**, *23*, 337–345.
(39) Bhushan, B.; Wei, G.; Haddad, P. *Wear* **2005**, *259*, 1012–1021.
(40) Huson, M.; Evans, D.; Church, J.; Hutchinson, S.; Maxwell, J.; Corino, G. *J. Struct. Biol.* **2008**, *163*, 127–136.
(41) Scofield, J. H. *J. Electron Spectrosc. Relat. Phenom.* **1976**, *8*, 129–138.

AM900337Z